WELDING RESEARCH

SUPPLEMENT TO THE WELDING JOURNAL, APRIL 1977

Sponsored by the American Welding Society and the Welding Research Council

Weldability of High Toughness Fe-12% Ni Alloys Containing Ti, Al or Nb

An Fe-12% Ni alloy with 0.25% Ti proves extremely weldable for cryogenic application, having weld and HAZ properties comparable with those of the wrought base metal

BY J. H. DEVLETIAN, J. R. STEPHENS AND W. R. WITZKE

ABSTRACT. Three exceptionally high-toughness Fe-12%Ni alloys designed for cryogenic service were welded using the GTA welding process. Evaluation of weldability included equivalent energy K_{Ieq} fracture toughness tests, transverse-weld tensile tests at −196 and 25 C (−321 and 77 F) and weld crack sensitivity tests.

The Fe-12%Ni-0.25%Ti alloy proved extremely weldable for cryogenic applications, having weld and heat-affected zone properties comparable with those of the wrought base alloy. The Fe-12%Ni-0.5%Al had good weld properties only after the weld joint was heat treated. The Fe-12%Ni-0.25%Nb alloy was not considered weldable for cryogenic use because of its poor weld joint properties at −196 C and its susceptibility to hot cracking.

Introduction

The need for alloys for cryogenic service has increased substantially during recent years. Transporting and storage of liquefied natural gas (which boils at −160 C or −255 F) is one of the primary areas that requires large amounts of alloys for cryogenic service. Iron base alloys that are currently in use or are being considered for cryogenic applications include Type 304 stainless steel, 9Ni steel, and 5Ni steel.[1] The Type 304 stainless steel is a high toughness, low strength alloy, while the 9Ni and 5Ni steels have somewhat lower toughness at high strength levels.

Results of an alloy development study at the University of California[2] showed that an experimental Fe-12%Ni-0.3%Ti alloy that had been heat treated to produce an extremely fine grain size exhibited a toughness at −196 C (boiling point of liquid nitrogen) equal to that of Type 304 stainless steel at a strength level of the stronger 9Ni steel. More recently, Witzke and Stephens[3] have identified several reactive metal additions which improve the −196 C (−321 F) toughness of the Fe-12%Ni alloy without the need for complex grain refining heat treatments. In order to utilize these experimental alloys at cryogenic temperatures, their ability to be welded without sacrificing a substantial degree of toughness and strength must be demonstrated.

The purpose of this investigation was to determine the relative weldability of the three most promising experimental Fe-12%Ni-reactive metal alloys identified in the literature.[3] The three alloys selected were: Fe-12%Ni-0.25%Ti; Fe-12%Ni-0.5%Al; and Fe-12%Ni-0.25%Nb.*

These alloys possess excellent combinations of tensile strength and fracture toughness at cryogenic temperatures. Welding by the gas tungsten arc (GTA) process was performed on 1 mm (0.039 in.) thick sheet and on 7 mm (0.276 in.) thick plate. The primary means of assessing the weldability of these experimental alloys involved equivalent energy K_{Ieq} fracture toughness testing. In addition, transverse-weld tensile tests, circular patch tests, and supplementary metallographic and electron microprobe evaluations were conducted.

Experimental Procedure

Materials

The Fe-12%Ni alloys used in this investigation were prepared from vac-

Paper to be presented at the 58th AWS Annual Meeting in Philadelphia, PA, during April 25-28, 1977.

J. H. DEVLETIAN is Assistant Professor, Department of Chemical Engineering and Materials Science, Youngstown State University, Youngstown, Ohio, and J. R. STEPHENS and W. R. WITZKE are with the National Aeronautics and Space Administration, Lewis Research Center, Cleveland, Ohio.

**All alloy compositions in this report are given in atomic percent. The symbol Nb for niobiom is used throughout this report instead of the U.S. customary Cb for colombium.*

uum processed Fe rod of 99.95 wt% purity, electrolytic Ni chips containing less than 100 weight ppm total interstitial impurities, and the reactive metals: Ti containing less than 5000 ppm interstitial impurities and Al and Nb with less than 100 ppm total of O, N, and C.

Ingots were prepared by nonconsumable arc melting of 1000 g charges in a 75 × 75 × 30 mm (2.95 × 2.95 × 1.18 in.) deep water cooled copper mold after evacuating and backfilling with argon to one-half atmosphere pressure. To adequately homogenize the ingots, each was given a minimum of four melts.

Two ingots of each alloy were hot rolled at 1100 C (2012 F) after annealing for ½ h at that temperature. The rolling procedure included 15% reductions per pass and 2 rolling passes per 5 minute reheat. For each alloy, the first ingot was rolled to a thickness of 1 mm while the second was rolled to 7 mm. These two sizes were selected because the 1 mm sheet could be a thickness used in the fabrication of commercial cryogenic containers while the 7 mm size was required for fracture toughness evaluation.

The 1 mm thick hot-rolled sheet was prepared for welding by shearing into 89 × 76 mm (3.5 × 3 in.) sections while the 7 mm thick hot-rolled plate was machined into 64 × 51 mm (2.5 × 2 in.) sections containing a double-V-groove as shown in Fig. 1(a). Approximately two-thirds of the 1 mm and 7 mm sections were heat treated to achieve maximum fracture toughness at −196 C prior to welding. This heat treatment varied for each alloy[3]: the Fe-12%Ni-0.5%Al was annealed for 2 h at 550 C (1022 F) in an argon atmosphere followed by a rapid brine quench. The Fe-12%Ni-0.25%Nb and Fe-12%Ni-0.25%Ti alloys were similarly quench-annealed at 820 and 685 C (1508 and 1265 F), respectively.

All specimens to be welded were grit blasted and cleaned in acetone. Following welding some of the welded specimens were postweld quench-annealed using the procedures described above.

Procedure

Welding. Full penetrating single-pass welds were deposited on all 1 mm thick sheet specimens using the autogenous GTA welding process with 200 cm^3/s (25.4 cfh) argon gas shielding. All of the 7 mm thick specimens were GTA welded in four passes (pass sequence is shown in Fig. 1(b)) using 2.3 mm (0.091 in.) diameter filler metal swaged from the base metal. Welding parameters for the 1 mm thick sheet ranged between 50-100 A, 9-11 V, and

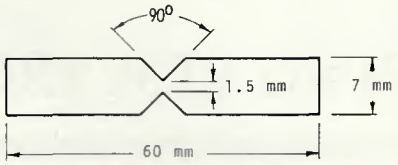

(a) WORKPIECE PREPARATION BEFORE WELDING.

(b) SUBSEQUENT AS-WELDED CONFIGURATION SHOWING WELD-PASS SEQUENCE.

Fig. 1—Gas tungsten arc (GTA) weld joint

150-250 mm/min (5.91-9.84 ipm) travel speed while those for the 7 mm thick specimens required 130-140 A, 11-13 V, and 100-150 mm/min (3.94-5.91 ipm) travel speed.

Weld cooling rates measured at 704 C (1300 F) were taken for each weld by plunging a 0.38 mm (0.015 in.) diameter W/W-26%Re thermocouple directly into the weld pool. Cooling curves for each weld were recorded on a continuous chart recorder. Three weld cooling rates ranging from 3 to 142 C/s (37 to 288 F/s) were investigated. Slow weld cooling rates were obtained by preheating the workpiece to 260 C (500 F). Extremely fast cooling rates were obtained by tightly clamping a 7 mm thick copper backing plate to the workpiece. Intermediate or normal weld cooling rates were obtained by allowing the weld metal to cool in air without preheating or backing material.

Fracture Toughness Test. Slow bend test specimens were used to determine the fracture toughness values for both the weld metal and heat-affected zone (HAZ). The test specimens were 50.8 × 10 × 6.4 mm (2 × 0.394 × 0.252 in.) notched Charpy bars. Two sets of bars without notches were first machined from the welded sections. Each bar was etched with 2% nital to reveal the weld location so that the notch on one set could be machined in the weld metal while the notch in the second set could be machined in the HAZ. Each specimen was then fatigue-cracked to an initial crack length-to-specimen width ratio (a/W) of approximately 0.4.

Testing was conducted in a 3-point bending apparatus immersed in a liquid nitrogen bath or at room temperature. The specimens were positioned between a 6.4 mm (0.252 in.) diameter center roller and two similar support rollers to provide a support span of 38.1 mm (1.5 in.). A crosshead speed of 1.3 mm/min (0.051 ipm) was used. A load/displacement curve was generated from the outputs of a load cell which supported the bend apparatus and a double cantilever clip-on displacement gage[4]. This gage sensed the crack opening displacement via the vertical movement of a ceramic rod riding on the bend bar.

The fracture toughness parameter K_{Ied} was determined from load/displacement curves using the K_{Ie} equation for a slow bend test specimen as given in ASTM Standard E399[4] as modified by the empirical Equivalent Energy Method[5]. The relation used for calculating the fracture toughness of a slow bend test specimen was:

$$K_{Ied} = [(SP_2\sqrt{A_1/A_2})f(a/W)]/BW^{3/2}$$

where: S = span; a = specimen crack depth; W = specimen width; B = specimen thickness; P_2 = any load on linear portion of load/displacement curve; A_2 = area under curve to P_2; A_1 = area under curve to maximum load; f(a/W) = value of power series for a/W from ASTM.[4] The fracture toughness data presented are generally values obtained from single tests.

Tensile Tests. Flat transverse-weld tensile specimens with reduced section dimensions of 1 by 6.3 mm (0.039 by 0.248 in.) and a gage length of 25.4 mm (1 in.) were tested at 25 and −196 C at a crosshead speed of 1.3 mm/min. Similar unwelded specimens also were tested to provide reference base metal properties.

Weld Cracking Test. The standard crack-susceptibility circular patch test (test no. 61 in[6]) was employed to determine the resistance of each alloy to hot and cold weld cracking. GTA welds were deposited along a 51 mm (2 in.) diameter circle on 1 mm thick sheets. Welding was done manually at room temperature.

Electron Microprobe. Microprobe analyses, using the specimen traverse technique, were conducted on the weld metal and HAZ to detect the presence and distribution of Ni, Al, Nb, and Ti in the Fe-12%Ni alloys.

Metallography. All welded joints were sectioned transversely for metallographic examination. Etchants employed included standard 2% nital to reveal the cellular solidification structure and a three-acid etchant consisting of 1 part by volume HF, 33 parts HNO_3 and 33 parts acetic acid in 933 parts H_2O to show the weld structure resulting from solid state transformation.

Results

The weldabilities of Fe-12%Ni alloys containing additions of Ti, Al or Nb were evaluated by equivalent energy K_{Ied} fracture toughness and transverse-weld tensile tests. Results from these tests are presented in Figs. 2 to 7. Unless otherwise indicated, all weld properties cited herein are for welds made

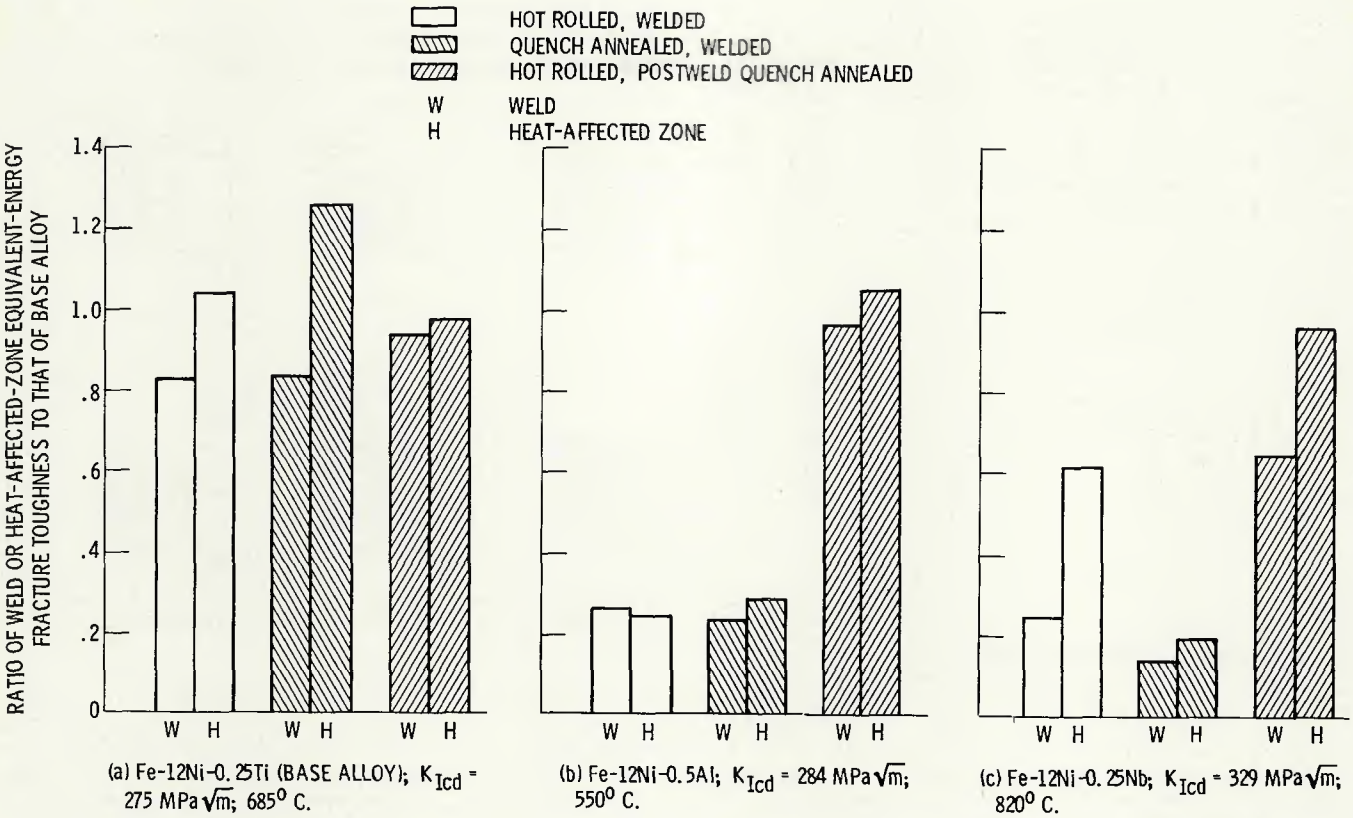

Fig. 2—Effects of pre- and postweld heat treatments on −196 C (−321 F) fracture toughness of welded Fe-12Ni alloys compared with that of the base metal heat treated for maximum toughness

under intermediate or normal cooling rates.

Fracture Toughness

At −196 C, the Fe-12%Ni-0.25%Ti alloy possessed high as-welded K_{Icd} fracture toughness values in both the weld metal and HAZ with or without preweld heat treatment (227 to 347 MPa$\sqrt{m}$). These toughness levels compared favorably with that of the base metal (275 MPa$\sqrt{m}$) which had been quench-annealed at 685 C (1265 F) for maximum toughness as shown in Fig. 2. Postweld heat treating was found to have little effect on the toughness of the weld or HAZ of this alloy. As shown in Fig. 3(a), minor increases in weld and HAZ fracture toughness values were observed as the weld cooling rate was increased.

For the Fe-12%Ni-0.5%Al alloy, at −196 C, the weld and HAZ fracture toughness values in the as-welded condition (with or without preweld heat treatment) were generally poor: 69 to 81 MPa$\sqrt{m}$ compared to 284 MPa$\sqrt{m}$ for the heat treated base metal, as shown in Fig. 2. However, postweld quench-annealing these welded specimens at 550 C (1022 F) effectively increased the weld and HAZ toughness values (275 and 300 MPa$\sqrt{m}$, respectively) to approximately the level of the base metal. As shown in Fig. 3(b), the weld cooling rate had no significant effect on weld or HAZ toughness of this alloy.

The as-weld fracture toughnesses of the Fe-12%Ni-0.25%Nb alloy at −196C were poor to medium: 47 to 205 MPa$\sqrt{m}$, compared to 329 MPa$\sqrt{m}$ for the quench-annealed base metal (Fig. 2). With postweld quench-annealing at 820 C (1508 F), the HAZ toughness value (320 MPa$\sqrt{m}$) was effectively raised to the level of the base metal, but the toughness of the weld (213 MPa$\sqrt{m}$) remained significantly below that of the base metal

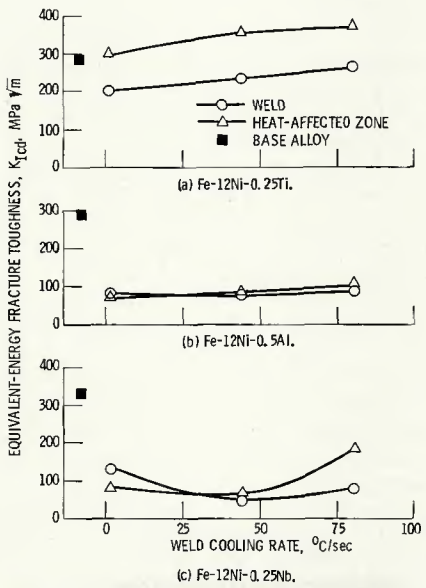

Fig. 3—Effect of weld cooling rate on the −196 C fracture toughness of Fe-12Ni alloys. (Reference base metal was heat treated for maximum toughness)

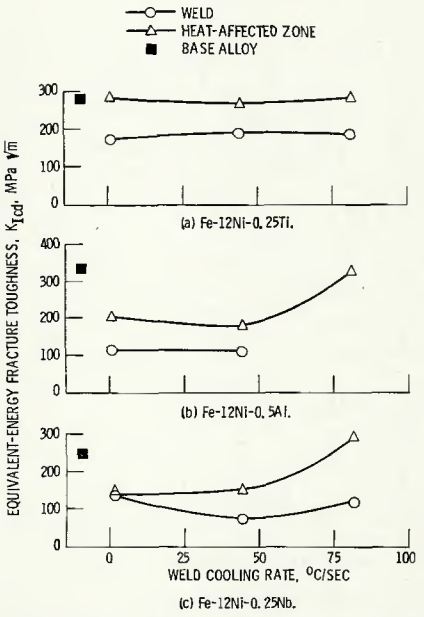

Fig. 4—Effect of weld cooling rate on 25 C (77 F) fracture toughness of Fe-12Ni alloys. (Reference base metal was heat treated for maximum toughness)

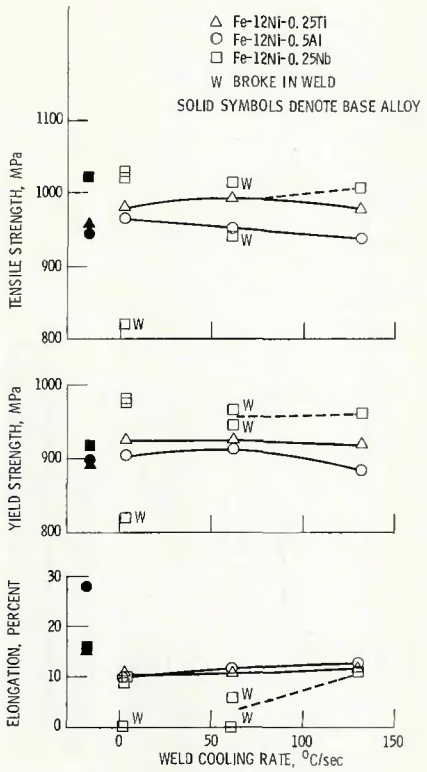

Fig. 5—Effect of weld cooling rate on transverse-weld tensile properties of Fe-12Ni alloys tested at −196 C. (Properties of base metal, heat treated for maximum toughness, are shown for comparison[3])

(329 MPa$\sqrt{m}$). As shown in Fig. 3(c), the weld cooling rate was found to have only a minor effect on toughness.

Fracture toughness trends observed at 25 C were similar to those at −196 C, as shown in Fig. 4. The Ti-containing alloy possessed relatively high weld and HAZ fracture toughness values (188 and 264 MPa$\sqrt{m}$, respectively) in

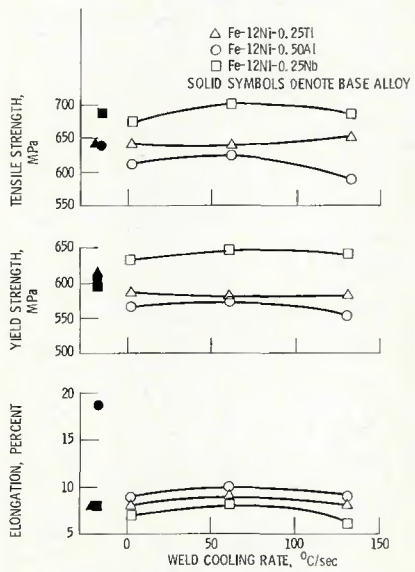

Fig. 7—Effect of weld cooling rate on transverse-weld tensile properties of Fe-12Ni alloys tested at 25 C. (Properties of base metal, heat treated to maximum toughness, are shown for comparison[3])

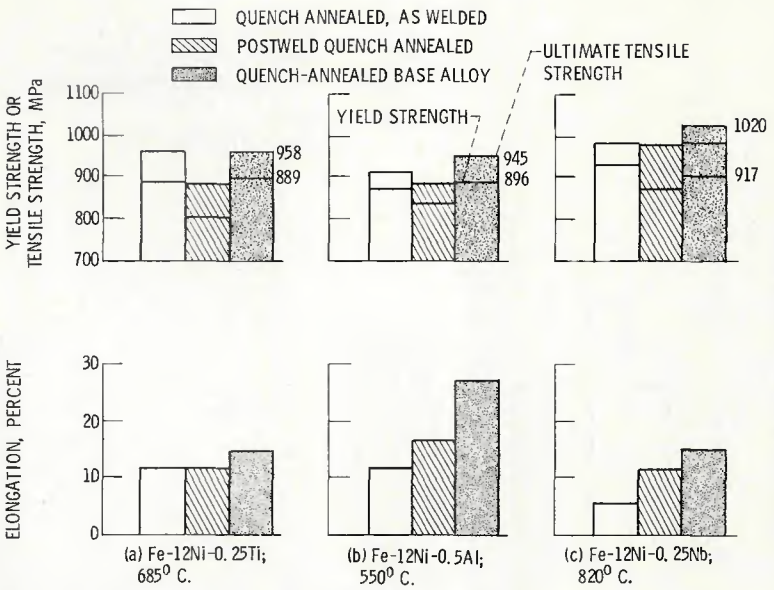

Fig. 6—Transverse-weld tensile properties of gas tungsten-arc welded, 1 mm (0.039 in.) thick Fe-12Ni alloys tested at −196 C, and quench-annealed at various temperatures

the as-welded condition compared to 276 MPa$\sqrt{m}$ for the quench-annealed base metal. The corresponding weld toughness values for the Al and Nb-bearing alloys at 25 C were significantly lower than their respective base metal toughness levels.

Tensile Properties

The transverse-weld tensile properties at −196 C of the Fe-12%Ni-0.25%Ti alloy (Fig. 5) compared closely with those of the quench-annealed base metal. Weld cooling rate did not affect properties, and all transverse-weld specimens failed outside the weld. Postweld quench-annealing of these specimens resulted in no major changes in tensile properties, as shown in Fig. 6.

At −196 C, the weld-joint tensile properties of the Fe-12%Ni-0.5%Al alloy (shown in Fig. 5) were comparable to those of the base metal except for tensile elongation. The weld-joint elongation of 12% was far below the 28% recorded for the base metal in the quench-annealed condition. All fractures of the transverse-weld tensile specimens occurred outside both the weld and HAZ. Weld cooling rate had no appreciable effect on tensile properties, as shown in Fig. 5. Postweld quench-annealing at 550 C resulted in a minor increase in elongation accompanied by corresponding decreases in tensile and yield strengths (see Fig. 6).

The weld-joint tensile properties of Fe-12%Ni-0.25%Nb at −196 C were comparable to those of the quench-annealed base metal only when the transverse-weld specimen failed outside the weld (Fig. 5). Tensile failures occurring within the weld zone resulted in lower and more erratic tensile properties. For example, the elongation and yield strength values of transverse-weld specimens failing outside the weld varied from 10 to 11% and 958 to 979 MPa (139 to 142 ksi), respectively, while those failing in the weld zone ranged from 0 to 6% elongation and 820 to 965 MPa (119 to 140 ksi) yield strength. Weld cooling rate appeared to have little effect on weld-joint properties. As shown in Fig. 6, postweld quench-annealing at 820 C tended to improve ductility and to decrease the occurrence of weld metal failures.

The weld-joint tensile properties at 25 C of the Fe-12%Ni alloys containing Ti, Al, or Nb (Fig. 7) displayed the following general similarities:

1. All transverse-weld tensile specimens failed outside the weld.
2. Weld cooling rate had virtually no effect on tensile properties.
3. Weld-joint properties for each alloy tended to parallel those of the quench-annealed base metal.
4. Postweld quench-annealing resulted in very little change in elongation accompanied by slight decreases in tensile and yield strengths.

Crack-Susceptibility of Welds

GTA welds made on 1 and 7 mm thick specimens of Fe-12%Ni-0.25%Ti and Fe-12%Ni-0.5%Al alloys were defect-free as evidenced by radiographic inspection. However, cracking problems were encountered when the 7 mm thick specimens of Fe-12%Ni-0.25%Nb alloy were GTA welded using filler metal of the same composition as that of the base metal. This alloy exhibited strong hot cracking tendencies during the first and second passes

Table 1—GTA Welding Transfer Efficiencies and Protection from Atmospheric Contamination

Alloy	Analyzed for Solute content, at. % Ni	Ti	Al	Nb	Interstitial content, ppm by weight C	N	O
Fe-12Ni-0.25Ti							
Base metal		0.26			160	12	16
Weld		0.21			144	13	14
Base metal	11.96				—	13	20
Weld	11.92				—	16	70
Fe-12Ni-0.5Al							
Base metal	12.00		0.45		189	6	29
Weld	11.94		0.41		145	8	38
Fe-12Ni-0.25Nb							
Base metal	12.02			0.22	132	20	14
Weld	11.96			0.21	56	24	92
Transfer efficiency across arc, %	99	81	91	95			

of the four-pass weld (welding sequence is shown in Fig. 1(b)). No cracking resulted when the relatively unrestrained 1 mm thick sheet specimens were GTA welded.

Standard circular patch tests[6], using the 51 mm diameter GTA weld circle, verified these hot-cracking observations. The Al and Ti-bearing alloys had excellent resistance to hot and cold cracking, while the Nb-bearing alloy showed extensive hot-cracking along the centerlines of each weld.

Chemistry/Metal Transfer Through Arc

High transfer efficiencies, (i.e., transfer of alloying elements from filler metal to weld) were obtained in this investigation for the major alloying elements Ni, Ti, Al, and Nb during 4-pass GTA welding, as shown in Table 1. Even Ti, which is one of the most difficult elements to transfer across a welding arc, was successfully transferred with an efficiency of 81%.

The GTA welding process effectively protected the molten weld pool from interstitial contamination from the atmosphere. A comparison of the O, N, and C contents between the weld metal and the adjacent base metal in Table 1 showed that the interstitial content was low in both of these regions.

Weld Microstructure

The solidification structures of all three Fe-12%Ni alloys (as revealed by etching in nital) were typically cellular over the wide range of weld cooling rates investigated (3 to 142 C/s) (37 to 288 F/s). In Fig. 8(a), each weld metal grain, which has grown epitaxially from the HAZ, contains the cellular substructure. Postweld quench-annealing to maximize toughness had little effect upon the solidification structure, as shown in Fig. 8(b).

Upon repolishing and etching these welds with the three-acid etchant to reveal the weld microstructures associated with solid state transformations during weld cooling, results showed only minimal effects from additions of Ti, Al, and Nb on the Fe-12%Ni base metal. From Fig. 9 (a-1, b-1 and c-1), the weld metal microstructures of Ti, Al, and Nb-bearing alloys in the as-welded condition are seen to be essentially all martensitic. X-ray diffraction studies of these alloy welds clearly indicated the presence of at least 99%, martensite with the remaining 1% attributed to retained austenite.

The wide range of weld cooling rates used in this investigation had no significant effect on the resulting martensitic structure. The only characteristic microstructural features resulting from the addition of Al, Nb, and Ti were the precipitation of interstitial compounds, which appear as widely scattered microscopic particles in Fig. 9.

The metallurgical condition of the workpiece prior to welding had no appreciable effect on the weld microstructure. Welds deposited on both hot-rolled sheet and quench-annealed sheet had essentially identical weld and HAZ microstructures, similar to those shown in Figs. 8 and 9, for all three alloys tested.

Postweld heat treating of the martensitic weld metal structures to attain maximum fracture toughness resulted in the several significant effects on microstructure. The Fe-12%Ni-0.25%Ti alloy weld was quench-annealed at 685 C (1265 F), which is in the ferrite plus austenite range. This weld microstructure (Fig. 9(a-2)) contains a fine laminated morphology of ferrite (light) and tempered martensite (dark). Postweld quench-annealing of the Fe-12%Ni-0.5%Al alloy weld at 550 C effectively tempered the as-welded martensitic structure, as shown in Fig.

(a) As welded.

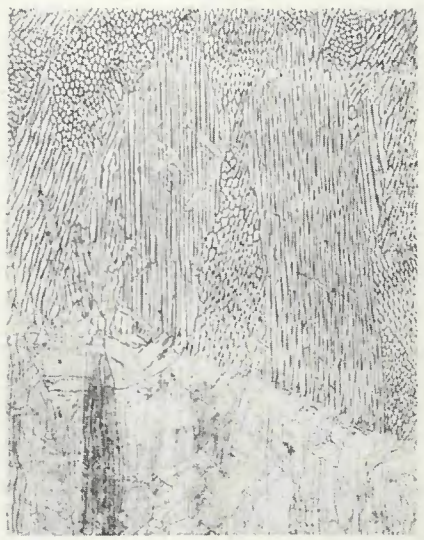

(b) Postweld quench annealed at 550° C.

Fig. 8—Typical cellular solidification structure of Fe-12Ni-0.5Al weld metal. Etchant, nital; ×100, reduced 29% upon reproduction

9(b-2). Quench-annealing the Fe-12%Ni-0.25%Nb alloy weld at 820 C (1508 F) produced a fine-grained martensitic structure, shown in Fig. 9(c-2).

Electron Microprobe Analyses

Results from microprobe scans across the welds of the three experimental alloys indicated that Ni segregated strongly at practically all solidification cell boundaries. For example, with the Fe-12%Ni-0.25%Nb alloy, Ni peaks occurred at every optically observed cell boundary (Fig. 10 shows a segment of the Ni and Nb scans). About 75% of the strong Nb peaks occurred at these same boundary locations. The sole noncorresponding Nb-peak in Fig. 10, indicated by the letter "A," occurred at a Nb-rich precipitate within a cell.

In the weld metal of the Al and Ti-

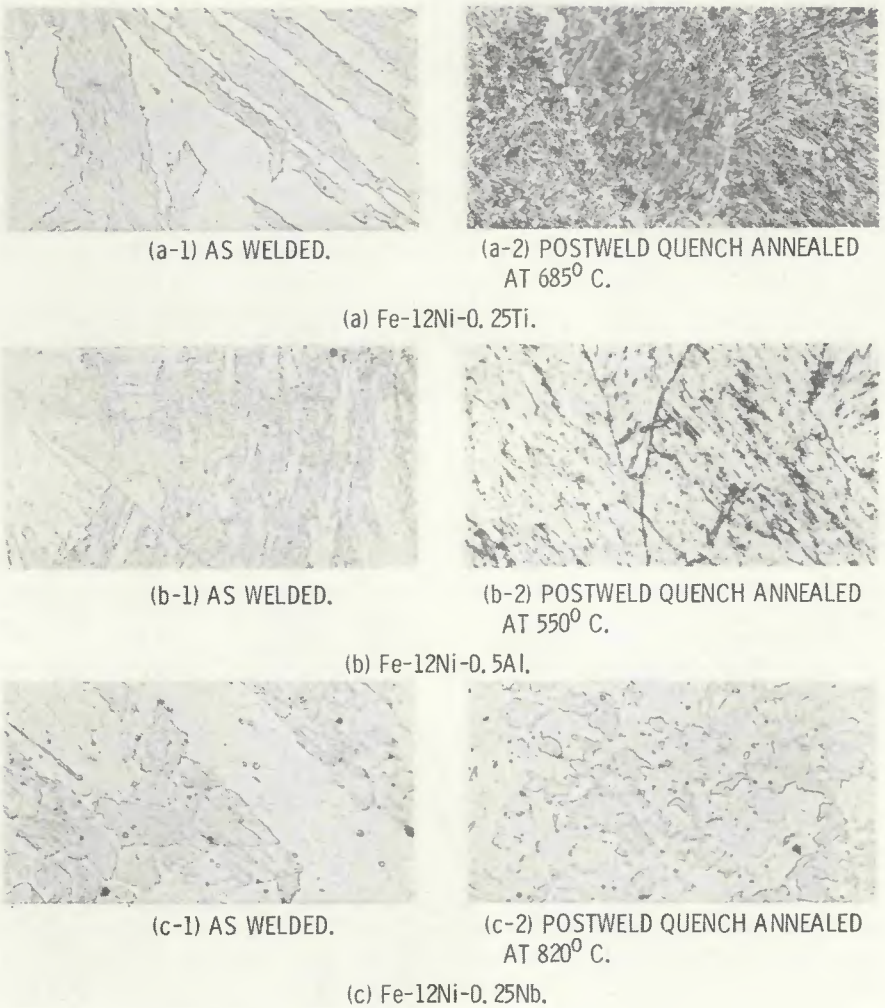

Fig. 9—Weld microstructures of Fe-12Ni alloys as-welded and postweld quench-annealed at 685, 550 and 820 C (1265, 1022 and 1508 F). Etchant, three acids; ×750, not reduced upon reproduction

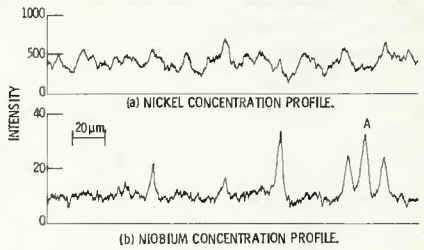

Fig. 10—Segment of electron microprobe line scan for nickel and niobium in gas tungsten arc welded Fe-12Ni-0.25Nb

bearing alloys, somewhat weaker Al and Ti peaks were detected at cell boundaries. Since the detection limit of these elements in the scanning mode was about 0.1% by weight, small concentration gradients of Ti, Al, and Nb between cell centers and peripheries could not be detected. No significant segregation of alloying elements was observed in the HAZ.

Discussion

Fracture Toughness

The most promising alloy from a weldability viewpoint is the Fe-12Ni-0.25Ti alloy. This alloy exhibited the highest weld metal and HAZ equivalent energy K_{Ied} fracture toughness values at 25 and −196 C in the as-welded condition. From Figs. 2, 3, and 4, the fracture toughness values of the weld zone and HAZ of this alloy were found to be about equivalent to that of the base metal which was quench-annealed at 685 C for maximum toughness.

It is extremely significant from a structural point of view that the HAZ retained the base metal toughness because the HAZ is an inherent part of the wrought base metal. The toughness of the HAZ cannot be changed except by postweld heat treatment which may, in many cases, be impractical or uneconomical. On the other hand, virtually any value of toughness may be obtained in the weld metal by simply choosing the appropriate filler metal composition. Thus, a high toughness alloy which has a high HAZ toughness in the as-welded condition is ideal for welding applications in the field where postweld heat treating is unfeasible.

This points up a potential commercial advantage of the Fe-12%Ni-0.25%Ti alloy over the Al and Nb-bearing alloys, which have poor as-welded toughness in the HAZ. Furthermore, the weld and HAZ toughness of the Ti-bearing alloy was unaffected by weld cooling rate (Figs. 3 and 4). As a result, welds could be made on practically any thickness of sheet or plate while still maintaining high toughness. Finally, a substantial reduction in cost of filler metal is derived without an appreciable loss in overall weld-joint toughness by using the Fe-12%Ni-0.25%Ti alloy filler metal to replace the more expensive Ni-base fillers, which are commonly used to weld Fe-9%Ni alloys[7].

For applications where the welds can be postweld heat treated to maximum toughness, then the Al-bearing alloy also becomes attractive. Although the weld and HAZ toughness values at −196 C of the Fe-12%Ni-0.5%Al alloy (Fig. 2) were poor in the as-welded condition, the toughness values after quench-annealing at 550 C were excellent, equaling that of the base metal. Therefore, all cryogenic structural applications using the Al-bearing alloy would require a postweld quench-annealing operation.

The most difficult weldability problems were encountered with the Fe-12%Ni-0.25%Nb alloy, which had the highest wrought alloy toughness of the three alloys investigated. Welds made from this alloy were not only found to be hot-crack sensitive and low in toughness but also inadequately responsive to postweld quench-annealing (Fig. 2). Clearly, welding of the Nb-bearing alloy would require development of a tough filler alloy for higher weld metal toughness.

Weld Cracking and Tensile Properties

The Ti and Al-bearing alloys have been shown to have good resistance to weld cracking, but the Nb-bearing alloy weld metal is plagued with a serious hot-cracking problem. Unless a suitable filler metal is developed, the general usefulness of the Fe-12%Ni-0.25%Nb alloy as a workable cryogenic steel would be severely limited.

Except for lower ductility in the Al-bearing alloy welds, the transverse-weld tensile properties at −196 C of the Ti and Al-bearing alloys were generally comparable to their respective quench-annealed base metal properties since all failures occurred in the base metal. Only the Nb-bearing alloy displayed erratic transverse-weld tensile properties (Fig. 5).

The scope of this work does not permit a full explanation of this behavior at −196 C. However, the low solubility of Nb in Fe (< 0.5 atomic %) compared to a solubility of approxi-

mately 8 atomic % Ti and > 20 atomic % Al in Fe may partially account for the erratic behavior of the Nb-bearing alloy. Cell boundary segregation of reactive metals in the weld was more prominent in the Nb-bearing alloy as evidenced by electron microprobe results. This suggests that the lower solubility of Nb in Fe led to this high level of segregation which may be a cause of the poor weld properties of this alloy.

The transverse-weld tensile properties at room temperature of the three alloys studied were all generally comparable to those of their respective base metal. Since all failures occurred outside the weld, design parameters for welded joints could be based on the lower strength base metal properties rather than those of the weld for room temperature applications.

Applicability of Other Welding Processes

In this investigation, the GTA welding process was used because it represented the "cleanest" commonly used process for welding sheet. The dense argon gas shielding adequately protected the molten Fe-12%Ni alloy welds from interstitial contamination (see Table 1). Although only the GTA welding process was studied here, some speculation can be made about the applicability of other welding processes.

Other welding processes which similarly protect the molten weld pool from the atmosphere should also be suitable—for example, gas metal arc, plasma arc, resistance, diffusion, or electron beam welding. However, potentially contaminating processes such as shielded metal arc, submerged arc, flux cored arc, or electroslag welding probably are not applicable for these alloys, since contamination would probably lead to low fracture toughness. Furthermore, the shielding gas required to weld Fe-12%Ni alloys must be dry and inert (such as dry argon or helium) but not reactive like CO_2 or O_2.

Conclusions

The effects of gas tungsten arc (GTA) welding on Fe-12%Ni alloys containing small additions of Ti, Al, or Nb were evaluated by equivalent energy K_{Ieq} fracture toughness and tensile studies of welded specimens at −196 and 25 C. Based on this study, the following conclusions were reached:

1. Fe-12%Ni-0.25%Ti alloy is weldable in virtually any thickness without preheating or postweld heat treatment and can achieve weld properties comparable to those of the base metal.
2. Fe-12%Ni-0.5%Al has good weldability but develops original toughness and strength only after a postweld heat treatment.
3. Fe-12%Ni-0.25%Nb alloy is not weldable due to severe hot-cracking tendencies and poor mechanical properties in the weld and HAZ.
4. The GTA welding process is an excellent method for welding Fe-12%Ni alloys.

Acknowledgments

The assistance of Mr. C. J. Osicka, J. P. King, and R. R. Martineau is gratefully acknowledged. Also, one author (J. H. D.) wishes to express appreciation to the NASA-ASEE Summer Faculty Program for financial support.

References

1. Kaufman, J. G., "Symposium on Properties of Materials for Liquefied Natural Gas Tankage," Special Technical Publication 579, American Society for Testing and Materials, Philadelphia, Pa., 1975.
2. Jin, S., Hwang, S. K., and Morris, J. W., Jr., "Comparative Fracture Toughness of an Ultrafine Grained Fe-Ni Alloy at Liquid Helium Temperature," *Metallurgical Transactions A*, Vol. 6A, (8) Aug. 1975, pp. 1569-1575.
3. Witzke, W. R., and Stephens, J. R., "Effect of Minor Reactive Metal Additions on Fracture Toughness of Iron—12-Percent-Nickel Alloy at −196 and 25 C," NASA TN D-8232, May 1976.
4. "Plane-Strain Fracture Toughness of Metallic Materials," ASTM Standard E-399-74, American Society for Testing and Materials, Philadelphia, Pa., 1974.
5. Witt, F. J., and Mager, T. R., "Procedure for Determining Bounding Values on Fracture Toughness K_{Ic} at Any Temperature," ORNL-TM-3894, Oak Ridge National Laboratory, Oak Ridge, Tenn., October 1972.
6. Randall, M. D., Monroe, R. E., and Rieppel, P. J., "Methods of Evaluating Welded Joints," DMIC Report 165, Battelle Memorial Institute, Defense Metals Information Center, Columbus, OH, December 1961.
7. *Nickel Alloy Steel Data Book*, Bulletin C, Section 4, p. 25, International Nickel Company, New York, NY, 1975.

The Welding Research Council

. . .extends a most cordial invitation to all 1977 AWS Convention and Welding Show attendees to be on hand for and to participate in the following events at the Philadelphia Civic Center on April 27 and 28:

- Wednesday, April 27—9:30 A.M. in Rooms 231 and 233. Session 10—Aluminum Alloy Weldments. . .58th AWS Annual Meeting technical program. Sponsored by the Aluminum Alloys Committee of WRC, this session will feature the following valuable and timely presentations by outstanding researchers:
  - —Iowa State University Fatigue Data Bank, by W. W. Sanders, Jr., Iowa State University.
  - —5083-0—The Cryogenic Aluminum Alloy—Welding Process vs. Performance, by F. G. Nelson and G. P. Yanok, Alcoa Research Laboratories.
  - —Fatigue of Aluminum Alloy Weldments in Marine Environments, by W. W. Sanders, Jr., and K. A. McDowell, Iowa State University.
  - —Fatigue Properties of 5456-H117 Aluminum Alloy Weldments, by D. Raghaven and M. Murphy, Bell Aerospce Division, Textron, Inc.
  - —Effects of Lack-of-Penetration and Lack-of-Fusion on the Fatigue Properties of 5083 Aluminum Alloy Welds, by J. D. Burk and F. V. Lawrence, Jr., University of Illinois.
- Thursday, April 28—9:30 A.M. and 2:00 P.M. in Rooms 230 and 232. Session B-5 (9:30 A.M.)—Diffusion Brazing and Session B-6 (2:00 P.M.)—Vacuum Brazing. . .Eighth International AWS Brazing Conference. Cosponsored by the Brazing Committee of WRC, both sessions will be symposiums featuring short presentations by recognized brazing authorities and informal participation by attending audiences. Scheduled speakers are as follows: Session B-5—S. Duvall, United Technologies; J. Zelahy, General Electric Co., R. Middleton (or C. Voehringer), United Technologies; M. Schwartz, Rohr Corp. Session B-6—F. Miller, Wall Colmonoy Corp.; W. Jones, Abar Corp.; M. Stern (or B. Ettinger), AMI; R. Blackburn, Aluminum Company of America.

The Weldability Committee of WRC will, with the American Society for Metals, cosponsor a symposium on "Weldability—Different Things to Different People" at 2:00 P.M. on Tuesday, April 26, in Plaza A at the Philadelphia Civic Center.